Published in final edited form as:
Macromolecules. 2012 May 8; 45(9): 3722–3731. doi:10.1021/ma300634d.

Reactivity ratios, and mechanistic insight for anionic ring-opening copolymerization of epoxides

Bongjae F. Lee[1,2,4], **Martin Wolffs**[1], **Kris T. Delaney**[1], **Johannes K. Sprafke**[1], **Frank A. Leibfarth**[1,3], **Craig J. Hawker**[1,2,3], and **Nathaniel A. Lynd**[1]

[1]Materials Research Laboratory, University of California, Santa Barbara

[2]Materials Department, University of California, Santa Barbara

[3]Department of Chemistry and Biochemistry, University of California, Santa Barbara

[4]Chemical Research Institute, Samsung Cheil Industries Inc., Republic of Korea

Abstract

Reactivity ratios were evaluated for anionic ring-opening copolymerizations of ethylene oxide (EO) with either allyl glycidyl ether (AGE) or ethylene glycol vinyl glycidyl ether (EGVGE) using a benzyl alkoxide initiator. The chemical shift for the benzylic protons of the initiator, as measured by ^{1}H NMR spectroscopy, were observed to be sensitive to the sequence of the first two monomers added to the initiator during polymer growth. Using a simple kinetic model for initiation and the first propagation step, reactivity ratios for the copolymerization of AGE and EGVGE with EO could be determined by analysis of the ^{1}H NMR spectroscopy for the resulting copolymer. For the copolymerization between EO and AGE, the reactivity ratios were determined to be $r_{AGE} = 1.31 \pm 0.26$ and $r_{EO} = 0.54 \pm 0.03$, while for EO and EGVGE, the reactivity ratios were $r_{EGVGE} = 3.50 \pm 0.90$ and $r_{EO} = 0.32 \pm 0.10$. These ratios were consistent with the compositional drift observed in the copolymerization between EO and EGVGE, with EGVGE being consumed early in the copolymerization. These experimental results, combined with density functional calculations, allowed a mechanism for oxyanionic ring-opening polymerization that begins with coordination of the Lewis-basic epoxide to the cation to be proposed. The calculated transition-state energies agree qualitatively with the observed relative rates for polymerization.

Introduction

A central undertaking of polymer chemistry is the development and syntheses of polymeric materials with prescribed physical properties and chemical functionalities. Copolymerization is a vitally important and powerful strategy for the synthesis of materials that allow properties to be tuned between those observed for two or more unique homopolymers. Among many polymerizable chemical functionalities, epoxide groups provide a versatile polymerizable functionality for designing materials via copolymerization. Polyethers, derived from epoxide-based monomers, are widely used materials in applications such as drug-delivery,[1] control of biocompatibility,[2] and are gaining more attention in other emerging applications, such as dye-sensitized solar cells [3] and lithium-polymer batteries.[4] For polyethers such as PEG, a central limitation is that functionalization is restricted to the chain ends, which limits the ability to modify and tune the parent structure.[5]

Correspondence to: C. J. Hawker (hawker@mrl.ucsb.edu), N. A. Lynd (lynd@mrl.ucsb.edu).

Supporting Information

An example transfer reaction to monomer is shown in Scheme S1, as well as additional ^{1}H and ^{13}C NMR spectra (Figures S1, and S2) as described in the text. This material is available free of charge via the Internet at http://pubs.acs.org.

To increase chemical functionality beyond the chain ends, and therefore the breadth of available physical properties in polyethers, copolymerizations between ethylene oxide and glycidyl ethers have been explored.[6-10] Allyl glycidyl ether (AGE) has been homopolymerized [11, 12] and copolymerized with ethylene oxide (EO).[8, 17] The advantages offered by AGE units are a low Tg (−78 °C),[11] lack of crystallinity, and an available alkene moiety for post-polymerization functionalization.[13-17] Due to the controlled nature of oxyanionic polymerization of epoxides combined with efficient thiolene click chemistry, the amount, and nature of functional groups on a polyether backbone can be accurately controlled.[6, 8, 13, 17-27] In addition to AGE, ethylene glycol vinyl glycidyl ether (EGVGE)[29,30] has been recently copolymerized with EO and provides a versatile vinyl ether moiety, which may form hydrolytically cleavable acetal linkage as well as undergo thiol-ene click reactions to form permanent covalent linkages as in the case of AGE.[31] For copolymerizations of AGE and EGVGE with ethylene oxide, the distribution of comonomer sequences was characterized as random based on a qualitative ^{13}C NMR spectroscopy analysis of triad resonances.[8, 31]

As for radical copolymerization, in polyether systems employing two or more epoxide monomers, such as P(EO-*co*-AGE) and P(EO-*co*-EGVGE), it is imperative to have a detailed understanding of the relative reactivities of the comonomers toward the living chain-end in order to effectively design copolyether materials. Heatley *et al.* systematically analyzed the relative reactivities between EO and propylene oxide (PO) by the resonances corresponding to comonomer triads in ^{13}C NMR spectra and matching the relative integrals to triad probabilities calculated based on the reactivity ratios. The resulting reactivity ratios were $r_{EO} = k_{EO/EO}/k_{EO/PO} = 3.1 \pm 0.4$ and $r_{PO} = k_{PO/PO}/k_{PO/EO} = 0.30 \pm 0.04$, which signifies that the reactivity of EO is greater than that of PO for both the EO and PO chain-ends. Based on these reactivity ratios, the EO/PO system produces copolymers that possess a gradient in composition with EO enriched near the initiator and PO enriched near the terminus. Since the seminal publication by Heatley *et al.*, which showed that EO was more reactive toward potassium alkoxide chain ends than PO, workers have often assumed that the reactivity of EO is generally greater than that of other epoxide monomers such as glycidyl ethers (GEs).[7-9, 31] Pang et al. have carried out copolymerizations of EO with ethoxyethyl glycidyl ether (EEGE) which resulted in $r_{EO} = 1.20 \pm 0.01$ and $r_{EEGE} = 0.76 \pm 0.02$.[32] These reactivity ratios, determined under specific reaction conditions (THF/DMSO 10/40 v/v, 60 °C), have lent some credence to the assumption that EO is more reactive than glycidyl ethers under certain reaction conditions.[33] However, this evidence is frequently not cited.[7-9]

Typically, determining reactivity ratios is labor-intensive and involves termination of multiple copolymerizations at low conversion (e.g., 5%) and characterization of the resultant copolymer composition, or monitoring the change in the relative comonomer concentrations for several copolymerizations at various comonomer molar ratios.[34] Herein, we report a new, simple method of determining reactivity ratios in copolymerizations of EO with functional GEs such as AGE and EGVGE. For copolymerizations of EGVGE or AGE with EO, we have identified resonances in the ^{1}H NMR spectra where the chemical shifts are sensitive to the identities of the first two monomers added to the initiator. Significantly, the functional glycidyl ether monomers were observed to be more reactive than EO under our reaction conditions with comonomer reactivity decreasing in the series EGVGE > AGE > EO. To understand these findings, a computational investigation into the polymerization mechanism *via* density functional theory (DFT) calculations revealed that the relative comonomer reactivities are determined primarily by the relative tendency of the epoxide monomer to coordinate with the potassium counter-ion. Combined, these results allow fundamental insights into the mechanism for anionic ring-opening polymerization of epoxides.

Results and Discussion

Copolymerizations of Ethylene Oxide and Allyl Glycidyl Ether

To investigate the copolymerization kinetics between ethylene oxide (EO) and functional glycidyl ethers (GEs), initial experiments explored the copolymerization of EO with allyl glycidyl ether (AGE). Initiation of the polymerization was achieved by the generation of potassium alkoxide initiators *in situ* through the titration of benzyl alcohol with a dilute solution of potassium naphthalenide;[35] an effective and convenient strategy for initiation of the anionic ring-opening polymerization of glycidyl ethers.[6, 12] This strategy was employed for copolymerizations of AGE with EO as shown in Scheme 1. Four poly[(allyl glycidyl ether)-*co*-(ethylene oxide)] (P(AGE-*co*-EO)) copolymers were polymerized at varying molar incorporation of EO: $[EO]_0/[AGE]_0$ = 0.77, 1.0, 3.0, and 7.5. Copolymerizations were carried out in tetrahydrofuran (THF) solution at 45 °C from a benzyl alcohol initiator for 20 hours. In all polymerizations, the resultant copolymer compositions corresponded to the initial monomer stoichiometry with size exclusion chromatography (SEC), ^{1}H, and ^{13}C NMR spectroscopy employed for structural characterization. The degree of polymerization, polydispersity indices, and molar ratios of EO to AGE are included in Table 1.

A representative ^{1}H NMR spectrum is shown in Figure 1 for $[EO]_0/[AGE]_0$ = 1.0. All peaks can be assigned to EO, AGE repeat-units, or *cis*-prop-1-enyl isomers,[12, 36] with the resonances corresponding to the benzylic protons of the initiator (Figure 1 inset, peak *), displaying a complicated array of singlets. Notably, the chemical shift of these individual singlets is dictated by the identity of the first two repeat units. As a result, the relative magnitudes of these benzyl singlets contain information on the reactivity of each monomer during the first two propagation steps. Definitive assignments of these four unique singlets could be made and correspond to the copolymers beginning with I–AGE–AGE, I–AGE–EO, I–EO–AGE, and I–EO–EO over a range of 4.53–4.56 ppm. The possible structures and related ^{1}H NMR spectra for the benzyl resonances are shown in Figure 2 for $[EO]_0/[AGE]_0$ = 0.77, 1.0, 3.0, and 7.5. For the ^{1}H NMR spectrum in Figure 2b at $[EO]_0/[AGE]_0$ = 1.0, a truly random copolymerization, where $r_{EO} = r_{AGE} = 1$, would result in an array of singlets with equal area. Experimentally, a bias toward AGE addition is apparent as evidenced by the increased intensity of the singlets corresponding to AGE addition to both the initiator and living EO or AGE chain ends. The fact that all four sequences can be identified and quantified enables the determination of the relative reactivity of the alkoxide species toward each monomer for the first two repeat units, and from this a simple kinetic model can be used to obtain the observed reactivity ratios.

Scheme 2 displays the initiation and first propagation step resulting in the four possible initial dimers. For polymerizations with $[I]_0 \ll [EO]_0$ and $[GE]_0$, and at the beginning of the polymerization ($t \approx 0$), the monomer concentrations may be approximated by their initial concentrations, i.e., $[EO] \approx [EO]_0$, and $[GE] \approx [GE]_0$. Assuming that the rate of polymerization is first order in monomer and polymer concentration, the change in concentration of all copolymers in the system beginning with the motif I–EO–EO is given by

$$\frac{d[\mathrm{I-EO-EO}]}{dt} = k_{E/E}[\mathrm{EO}]_0[\mathrm{I-EO}] \quad (1)$$

where $k_{E/E}$ is the propagation rate constant of EO reacting with I–EO. The approximation of using the initial concentration of EO is valid because the entire concentration of copolymers beginning with I–EO–EO is determined during the initial stage of the polymerization while $[EO] \approx [EO]_0$. Similar equations can be written for each category of copolymer that begins

with each dimer. The ordinary differential equations can be solved for each category of copolymer, as well as for the immediate products of initiation: I–EO, and I–GE. Taking the ratio of [I–GE–…] to [I–EO–…] gives

$$\frac{[\mathrm{I-GE-\ldots}]}{[\mathrm{I-EO-\ldots}]}=\frac{k_G[\mathrm{GE}]_0}{k_E[\mathrm{EO}]_0} \quad (2)$$

If the initial molar ratio of comonomers $[EO]_0/[GE]_0$ is known, then the reactivity ratio of the monomers towards the initiator can be determined by taking the appropriate ratio of integrals of the benzyl singlets from Figure 2. Carrying out the same analysis for the second monomer addition to I–EO and I–GE yields the following simple expressions for extracting the ratios of propagation rate constants of each monomer to an ethylene oxide chain end ($k_{E/E}$ or $k_{E/G}$), or to a glycidyl ether (GE) chain end ($k_{G/G}$ or $k_{G/E}$):

$$\frac{[\mathrm{I-EO-GE-\ldots}]}{[\mathrm{I-EO-EO-\ldots}]}=\frac{k_{E/G}}{k_{E/E}}\frac{[\mathrm{GE}]_0}{[\mathrm{EO}]_0} \quad (3)$$

$$\frac{[\mathrm{I-GE-GE-\ldots}]}{[\mathrm{I-GE-EO-\ldots}]}=\frac{k_{G/G}}{k_{G/E}}\frac{[\mathrm{GE}]_0}{[\mathrm{EO}]_0} \quad (4)$$

From the ratios of the integrals for the signals due to the benzylic protons, we can extract the ratio of propagation rate constants of AGE and EO reacting with a primary alkoxide at an EO chain-end ($k_{E/G}/k_{E/E}$), and the ratio of rate constants for AGE and EO reacting with the secondary alkoxide at an AGE chain-end ($k_{G/G}/k_{G/E}$) can be determined. These ratios are related to the reactivity ratios through the following definitions: $r_E = k_{E/E}/k_{E/G}$, and $r_G = k_{G/G}/k_{G/E}$.

The integrals of the individual benzyl singlets were evaluated by fitting four Lorentzian functions to the ^{1}H NMR data. The cumulative fits to the data are shown in Figure 2 along with the individual Lorentzian components of the fit. In general, the fits to the array of benzyl peaks were quantitative (e.g., 0.2% residual error for $[EO]_0/[AGE]_0 = 1.0$, Figure 2b) and accurate individual integrals for the benzyl singlets could be extracted. The ratios of rate constants could then be determined using equations 2-4 for the samples in Table 1. Under the copolymerization conditions (THF at 45 °C) and for the reaction of the potassium benzoxide initiator with AGE and EO, we obtained a ratio of initiation rate constants of k_G/k_E =2.20 ± 0.20 (G = AGE, and E = EO) were obtained. For the ratio of propagation rate constants with the primary alcohol of an EO chain-end, similar analysis yielded a reactivity ratio of $r_E = k_{E/E}/k_{E/G}$ = 0.54 ± 0.03. Finally, for the reaction with the secondary alcohol of an AGE chain-end, a reactivity ratio of $r_G = k_{G/G}/k_{G/E}$ = 1.31 ± 0.26 was calculated. We note that the EO/AGE system is nearly an *ideal* copolymerization with $r_G \times r_E$ close to 1, which is a general characteristic of ionic copolymerizations.[37] However, the resultant comonomer sequence based on these reactivity ratios is slight gradient copolymer with AGE enrichment at the start of the polymer chain.

To gain fundamental insight into the reactivity ratios, transition-state density functional calculations of the ring-opening mechanism were performed. It should be noted that minimum energy barriers do not translate directly into reaction rates, since there is no information about path degeneracy or dynamics, but the barrier energetics can nevertheless provide insight into trends in preferential reactivity. The calculations reported here refer to transitions in vacuum and were performed using the Gaussian 03 [38] software package with the 6-31G(d) basis set,[39] and the B3LYP approximation for the exchange-correlation functional.[40] Minimum-energy transition states were obtained using Berny optimization,

[41] and all transition states were verified to have exactly one unstable vibrational mode. All transition states have an imaginary frequency of ca. 450 cm^{-1} in the reaction coordinate, indicating similar curvatures of the potential-energy landscape at the saddle point.

Initially, the transition states for the first monomer attachment of ethylene oxide (EO) and allyl glycidyl ether (AGE) to the potassium alkoxide initiator (I) was studied. From the analysis it was found that the I–EO and I–AGE reactions have minimum-energy barriers of 14.8 and 11.8 kcal/mol, respectively with the 3.0 kcal/mol reduction in transition state energy arising from both the increased coordination of the AGE monomer to the potassium counter-ion, which contributes 1.0 kcal/mol, and the increased Lewis basicity of the AGE epoxide ring due to electron donation from the allyl ether substituent, which contributes another 2.0 kcal/mol decrease in transition state energy relative to EO addition. For the reaction of the second monomer all four combinations: I–EO–EO, I–EO–AGE, I–AGE–EO, and I–AGE–AGE were considered. Again, the transition state for AGE addition was found to have a lower activation barrier than EO due to the same increase in Lewis basicity and bidentate coordination of AGE to the potassium counter-ion as mentioned previously. For the formation of I–EO–EO, an activation barrier of 19.7 kcal/mol was determined whereas for I–EO–AGE it was 13.9 kcal/mol. For the formation of I–AGE–EO and I–AGE–AGE, activation barriers of 22.6 and 14.4 kcal/mol were determined. These computational results are qualitatively consistent with the experimental ^{1}H NMR observations in which the addition of AGE occurs faster than EO to the living polymer chain for both the initiator and chain ends. These results and the representations of the optimized structures and transition states are presented in Figure 3.

Copolymerizations of Ethylene Oxide and Ethylene Glycol Vinyl Glycidyl Ether

In order to further test this strategy for determining reactivity ratios and lend greater credence to the observation that glycidyl ethers can be more reactive than EO in anionic ring-opening polymerization, several poly[(ethylene glycol vinyl glycidyl ether)-*co*-(ethylene oxide)] (P(EGVGE-*co*-EO)) copolymers were synthesized at various monomer feed ratios, $[EO]_0/[EGVGE]_0$. Ethylene glycol vinyl glycidyl ether (EGVGE) was first synthesized by reacting ethylene glycol monovinyl ether with epichlorohydrin under basic conditions with fractional distillation providing EGVGE in purities greater than 99% as measured by gas chromatography (GC). The monomer purity was determined to be an important consideration in carrying out copolymerizations without chain-transfer side-reactions to the monomer (see Scheme S1 in Supporting Information). Monomer purities above 99% were required to suppress chain-transfer; below 99% purity, chain-transfer could be observed in ^{1}H NMR spectra of the copolymers (see Figure S1 in Supporting Information).[42] Immediately prior to use, the EGVGE was degassed by freeze-pump-thaw and the EGVGE and EO were then copolymerized under identical conditions to those for EO and AGE (Scheme 3, and Table 2).

As with the EO/AGE system, the relative intensities of the four resonances due to the benzyl protons changed gradually with changes in $[EO]_0/[EGVGE]_0$, which demonstrated that the chemical shift of the benzyl resonances was sensitive to the identity of the first two repeat units added to the benzyl alkoxide initiator (Figure 4). The four signals between 4.51–4.55 ppm were assigned to the benzyl end-group protons on copolymers belonging to one of four copolymers differentiated by the sequence of the first two repeat units, (1) I–EO–EO, (2) I–EO–EGVGE, (3) I–EGVGE–EO, and (4) I–EGVGE–EGVGE. As in the case of EO/AGE, fitting the four singlets provided a means to accurately resolve and integrate the relative population of copolymers belonging to each of the four categories. The benzyl resonances, along with the cumulative fit, and individual Lorentzian components of the fits are shown in Figure 5. Quantifying the integral values for the benzyl resonances in Figure 5b–d gave a ratio of initiation rate constants for the reaction of EGVGE (G) and EO (E) with the

potassium benzoxide initiator of $k_G/k_E = 5.22 \pm 1.30$, showing that EGVGE was thus strongly preferred by the potassium alkoxide initiator over EO. For a random copolymerization with $r_G = r_E = 1$, and $[EO]_0/[EGVGE]_0 \approx 1$, the integrals of each benzyl singlet would be expected to be equal. Instead, a strong bias toward adding EGVGE monomer was observed in Figure 5a where $[EO]_0/[EGVGE]_0 = 0.98$. The I–EGVGE–EGVGE motif (peak 4) is the most prevalent mode of initiation for the majority of polymers in the system, with virtually no detectible chains beginning with the I–EO–EO sequence. For the addition of EGVGE (G) and EO (E) to the primary alcohol of an EO chain end the ratio of propagation rate constants is $k_{E/G}/k_{E/E} = 3.30 \pm 0.88$, and the ratio of propagation rate constants to the EGVGE chain-end is $k_{G/G}/k_{G/E} = 3.50 \pm 0.90$. These reactivity ratios portray a more than three-fold preference for EGVGE over EO with $r_G = 3.50 \pm 0.90$ and $r_E = 0.32 \pm 0.10$. As is characteristic for ionic copolymerizations, the product of the reactivity ratios is consistent with an *ideal* copolymerization, i.e., $r_G \times r_E = 1.1$.

The reactivity ratios for AGE/EO and EGVGE/EO indicate that the addition of these functional glycidyl ether monomers to the initiator and living chain-end is favored over EO addition. This suggests that copolymerizations of EO with AGE or EGVGE result in gradient-type copolymers where the functional glycidyl ether is consumed early in the polymerization and the resulting repeat units are enriched near the initiator. To investigate the composition as a function of time, several identical copolymerizations ($[EO]_0/[EGVGE]_0 = 3.35$) were carried out for different duration and the resulting repeat units were determined using ^{1}H NMR spectroscopy. The degree of polymerization for EO and EGVGE repeat units incorporated into the copolymer are shown in Table 3 and plotted in Figure 6 as a function of polymerization time. Although the molar concentration of EO was 3.35 times that of EGVGE, EGVGE repeat units were incorporated into the copolymer at approximately the same rate as EO. Assuming first order kinetics in monomer concentration, this nearly equal rate of propagation indicates that the rate constant for EGVGE propagation is approximately three times that for EO, i.e. $r_G \approx 3$ where $r_G \times r_E \approx 1$. This is in excellent agreement with the reactivity ratios determined by the method described above: $r_G = 3.50 \pm 0.90$, and $r_E = 0.32 \pm 0.10$. Under these conditions, the EGVGE was quantitatively consumed after 20h at which time the EO conversion was 40%. Quantitative conversion of EO required approximately 72 hours. In addition, a numerical calculation of comonomer propagation using these reactivity ratios clearly reproduces the experimental compositional drift portrayed in Figure 6.

Based on the reactivity ratios determined by ^{1}H NMR spectroscopy in Figure 5 and the drift in copolymer composition during the polymerization, it is apparent that the copolymerization of EO and EGVGE does not result in random copolymers under our polymerization conditions, with reactivity ratios that vary significantly from those expected. [31] The comonomer sequence of this actually results in a pseudo-block copolymer of poly[(ethylene glycol vinyl glycidyl ether)-*grad*-(ethylene oxide)]-*b*-poly(ethylene oxide) with a long stretch of pure EO repeat units of ca. 150 repeat units near the terminus. As further support of the relative reactivities, a T_m emerges due to the long, nearly pure PEO segment that arises late in the copolymerization. We note that the preference of EGVGE over EO is stronger than that for AGE over EO, which also corresponds qualitatively to the trends determined from our DFT calculations of the transition state energies ($\Delta E^{\ddagger}$) for I–EGVGE formation at 10.6 kcal/mol, which is much lower than that for I–EO and I–AGE formation at 14.8 kcal/mol and 11.8 kcal/mol, respectively. This result is intuitively expected since the binding of EGVGE to the potassium ion is likely to three oxygen atoms, which should decrease the energy of the transition state even more than for AGE coordination (two oxygens).

For the copolymerization of EGVGE and EO, it is also interesting that the propagation of EO proceeded at a retarded rate relative to an EO homopolymerization even after complete consumption of EGVGE. Based on our proposed polymerization mechanism presented in Figure 3, where coordination of the epoxide to the potassium counter-ion is a vital component, we propose that the copolymerization exists in a state of dynamic equilibrium between coordination of the counter-ion with the comonomers and the polymer backbone. In the case of P(EO-*co*-EGVGE), the EGVGE-rich segments in the polymer backbone are likely to provide an excellent coordinating environment for the potassium counter-ion, and thus decrease the likelihood that unreacted EO monomers coordinate and react with the chain end.

Numerous investigations of the copolymerization of functional glycidyl ethers with ethylene oxide have recently been reported,[7-10, 31, 33] with most of the reports concluding that the sequence distribution of the copolymers was random based on triad analysis in ^{13}C NMR spectroscopy. No comparison was made, however, with reactivity ratio dependent triad probabilities derived by Heatly *et al.*[33] and others [43a–c]. The mere appearance of triad resonances provides insufficient information on the sequence distribution to assign a copolymerization as characteristically random or not (see Figure S2 in Supporting Information). In contrast, the simple but powerful method reported herein in which a single ^{1}H NMR experiment can provide not only reactivity ratios, but also the relative reactivities of the comonomers toward the initiator, is a direct measurement of the ratios of propagation rate constants at the beginning of the copolymerization. As a result, this new technique provides a more direct and conclusive spectroscopic measurement than the specific, qualitative ^{13}C NMR spectroscopy-based method adopted by others for copolymerizations of EO and glycidyl ethers.[7-10, 31, 33]

Conclusions

The use of benzyl alcohol as an initiator in the copolymerization of EO with GEs such as AGE and EGVGE forms the basis for a new approach to understanding the nature of copolymerization of epoxide derivatives. The benzyl CH_2 group provides a unique signal in the ^{1}H NMR spectrum with a chemical shift that is sensitive to the identity of the first two monomer units. Utilizing a simple kinetic model, reactivity ratios can be directly extracted from the integration values for this group in the resulting P(EO-*co*-AGE) and P(EO-*co*-EGVGE) copolymers. A surprising result of this analysis was that AGE and EGVGE were determined to be more reactive than EO under our reaction conditions. For the EO/AGE system, the reactivity ratios were $r_G = 1.31 \pm 0.26$ and $r_E = 0.54 \pm 0.03$ while the EO/EGVGE system showed an even greater bias towards addition of the glycidyl ether: $r_G = 3.50 \pm 0.90$ and $r_E = 0.32 \pm 0.10$. DFT calculations were carried out to investigate the mechanism of anionic ring-opening polymerization by potassium alkoxides with the rate-determining step of the polymerization proposed to be the coordination of the epoxide monomer to the counter-ion with the relative rates of reactivity being proportional to the relative affinities of the epoxide comonomers toward the potassium cation. The trends in transition state energies are consistent with the experimental observation of the faster addition of AGE and EGVGE to the potassium alkoxide chain end than that of EO, with the relative reactivities in the order of EGVGE > AGE > EO. The spectroscopic method, and conceptual framework developed herein provide vital tools for investigating the synthesis of copolyether materials by the anionic ring-opening polymerization of epoxides.

Experimental

Characterization

^{1}H NMR spectroscopy was carried out on a Bruker AC 500 spectrometer in deuterated chloroform ($CDCl_3$). Size exclusion chromatography (SEC) was performed on a Waters chromatograph with four Viscotek columns (two I-MBHMW-3078, I-series mixed bed high molecular weight columns and two I-MBLMW-3078, I-series mixed bed low molecular weight columns) for fractionation, a Water 2414 differential refractometer and a 2996 photodiode array detector for detection of eluent, and chloroform with 0.1% triethlyamine at room temperature was used as the mobile phase. Gas chromatography was carried out on a Shimadzu GC-2014 using a flame ionization detector and a Restek column (SHRXI-5MS) for separation. DSC measurements were performed using a TA Instruments Q2000 MDSC (modulated differential scanning calorimeter) with 50-position auto-sampler and mass flow control in the temperature range from −80 to 120°C at heating rates of 10 K/min and cooling rates of −5 K/min under nitrogen.

Materials

All chemicals were used as received from Sigma-Aldrich unless otherwise specified. THF was collected from a dry solvent system and used immediately thereafter. Benzyl alcohol was dried over calcium hydride and distilled before titration with potassium naphthalenide in THF (0.3 M). Ethylene oxide (EO) was degassed through several freeze-pump-thaw cycles and distilled to a flame-dried buret immediately before use. Potassium naphthalenide was prepared from potassium metal and recrystallized naphthalene in dry THF and allowed to stir with a glass-coated stir-bar for 24 h at room temperature before use. Allyl glycidyl ether was purchased from TCI-America, Inc., degassed through several freeze-pump-thaw cycles, distilled from butyl magnesium chloride to a buret for storage.

Synthesis of Ethylene Glycol Vinyl Glycidyl Ether (EGVGE)

An alternative synthesis of EGVGE was reported previously by Shostakovskii,[29] and recently by Mangold et al.[31] Ethylene glycol vinyl ether (20 g, 230 mmol) and epichlorohydrin (42 g, 450 mmol) were placed in a 500 ml round-bottom flask sitting on an ice bath, and the mixture was stirred with a magnetic stir-bar. Sodium hydroxide (230 mmol) was slowly added on the mixture at 0 °C to avoid generating excess heat. After three hours, the reaction flask was moved into a 50 °C oil bath and stirred for additional 12 hours. After cooling of the reaction mixture, the sodium chloride precipitate was filtered and the liquid was washed several times with water. Excess epichlorohydrin and residual moisture were removed by a rotary evaporator and overnight *in vacuo*. The resulting pale-orange liquid was then distilled under reduced pressure to yield the desired colorless liquid (95% yield, 99+% purity by GC). ^{1}H NMR of EGVGE (500 MHz, $CDCl_3$): δ 2.58/2.76 (doublet of doublets, C$\underline{H}_2$–*epoxide*), 3.11–3.13 (m, C$\underline{H}$–*epoxide*), 3.39/3.41 (doublet of doublets, −C$\underline{H}_2$–O-CH_2–CH_2–O–CH=CH_2), 3.68–3.83 (broad m, −C$\underline{H}_2$–O-CH_2–CH_2–O–CH=CH_2 and −CH_2–O-C$\underline{H}_2$–C$\underline{H}_2$–O–CH=CH_2), 3.98/4.16 (doublet of doublets, −O–CH=C$\underline{H}_2$), (doublet of doublets, −O–C$\underline{H}$=CH_2).

Synthesis of poly[(allyl glycidyl ether)-*co*-(ethylene oxide)]

All polymerizations were carried out on a Schlenk line in custom thick-walled glass reactors fitted with ACE-threads under an inert argon atmosphere. The reactors were fitted with a buret containing a pre-measured quantity of THF, a flexible connector to a buret containing ethylene oxide on ice at 0 °C, a glass arm containing a port for a 6mm puresep septum, and connectors to the Schlenk line. The reactors were flame-dried under vacuum and refilled with argon five times. Under a 7 kPa positive argon pressure atmosphere, THF drawn from a

solvent purification system was introduced by opening the threaded stopcock on the attached buret. Benzyl alcohol initiator was added by gas-tight syringe through a 6mm puresep septum. Potassium naphthalenide (0.3M in THF) was added drop-wise by cannula until a light green color persisted in solution, indicating complete deprotonation of the benzyl alcohol initiator. Ethylene oxide was added by lifting the cold buret and allowing the ethylene oxide to drain into THF solution while allyl glycidyl ether was simultaneously added *via* gas-tight syringe. Due to concern about the order of monomer addition affecting the determination of reactivity ratios, a second procedure was used: Benzyl alcohol was added to a separate vessel, titrated with potassium alkoxide, and then added to the pre-mixed solution of ethylene oxide and allyl glycidyl ether. No difference in reactivity ratios was evident following either method indicating that initiation was slow enough such that the order of monomer addition did not affect the relative intensities of benzyl end-group resonances.

^{1}H NMR of Poly(EO-*co*-AGE) (500 MHz, $CDCl_3$): δ 1.55 (d, −O–CH=CH–C$\underline{H}_3$), 3.47–3.72 (broad m, −C$\underline{H}_2$–C$\underline{H}$–O–C$\underline{H}_2$–C$\underline{H}$(C$\underline{H}_2$–O–CH_2–CH=CH_2)–O– and −C$\underline{H}_2$–C$\underline{H}$–O–C$\underline{H}_2$–C$\underline{H}$(C$\underline{H}_2$–O–CH=CH–CH_3)–O–), 3.79/3.87 (two broad peaks, −CH_2–CH(C$\underline{H}_2$–O–CH=CH–CH_3)–O–), 4.01 (d, −O–C$\underline{H}_2$–CH=CH_2), 4.38 (m, −O–CH=C$\underline{H}$–CH_3), 4.53–4.56 (four singlets, Ph-C$\underline{H}_2$–O–), 5.18/5.28 (doublet of doublets, −O–CH_2–CH=C$\underline{H}_2$), 5.91 (m, −O–CH_2–C$\underline{H}$=CH_2), 5.97 (d, −O–C$\underline{H}$=CH–CH_3), 7.30 (overlap with residual $CHCl_3$, 1H on $\underline{Ph}$–CH_2–O–), 7.36 (s, 4H on $\underline{Ph}$–CH_2–O–).^{13}C NMR of Poly(EO-*co*-AGE) (125 MHz): δ 70.9 (−$\underline{C}H_2$–$\underline{C}H_2$–O–$\underline{C}H_2$–CH($\underline{C}H_2$–O–CH_2–CH=CH_2)–O–), 72.0 (−O–$\underline{C}H_2$–CH=CH_2), 79.4 (−CH_2–$\underline{C}$H(CH_2–O–CH_2–CH=$\underline{C}H_2$)–O–), 100.3 (−O–CH=$\underline{C}$H–CH_3), 116.3 (−O–CH_2–CH(CH_2–O–CH_2–CH=$\underline{C}H_2$)–O–), 127.5/128.6 (5C, $\underline{P}$h–CH_2–O–), 135.6 (−CH_2–CH(CH_2–O–CH_2–$\underline{C}$H=CH_2)–O–), 138.8 (1C, $\underline{P}$h–CH2–O–), 146.8 (−CH_2–CH(CH_2–O–$\underline{C}$H=CH–CH_3)–O–).

Synthesis of poly[(ethylene glycol vinyl glycidyl ether)-*co*-(ethylene oxide)]

All polymerizations were carried out on a Schlenk line in custom thick-walled glass reactors fitted with threaded ACE-threads under an argon atmosphere. The reactors were dried under vacuum then refilled with argon five times. Under an argon atmosphere, benzyl alcohol initiator was added by gas-tight syringe through a 6-mm puresep septum. THF was then added by opening the valve of the already-connected burette on the reactor. The potassium alkoxide initiator was formed by titration of benzyl alcohol with potassium naphthalenide under argon until a green color persisted in solution indicating the deprotonation of all alcohols. After adding EGVGE and EO simultaneously, polymerizations were carried out at 45 °C for 10–72 h and terminated with isopropanol. Polymers were precipitated in hexane and dried *in vacuo* before characterization.

^{1}H NMR of Poly(EGVGE) (500 MHz, $CDCl_3$): δ 3.54–3.71 (broad m, −O–C$\underline{H}_2$–C$\underline{H}$(CH_2–O–C$\underline{H}_2$–C$\underline{H}_2$–O–CH=CH_2)–O–), 3.81/3.82 (two broad peaks, −O–CH_2–CH(C$\underline{H}_2$–O–CH_2–CH_2–O–CH=CH_2)–O–), 4.00/4.19 (doublet of doublets, −O–CH=C$\underline{H}_2$), 4.47–4.57 (multiple s, Ph–C$\underline{H}_2$–O–), 6.49 (m, −O–C$\underline{H}$=CH_2), 7.32 (overlap with residual $CHCl_3$, 1H on $\underline{Ph}$–CH_2–O–), 7.38 (s, 4H on $\underline{Ph}$–CH_2–O–). ^{1}H NMR of Poly(EGVGE-*co*-EO) (500 MHz, $CDCl_3$): δ 3.54–3.71 (broad m, −C$\underline{H}_2$–C$\underline{H}$–O–C$\underline{H}_2$–C$\underline{H}$(CH_2–O–C$\underline{H}_2$–C$\underline{H}_2$–O–CH=CH_2)–O–), 3.81/3.82 (two broad peaks, −CH_2–CH(C$\underline{H}_2$–O–CH_2–CH_2–O–CH=CH_2)–O–), 4.00/4.19 (doublet of doublets, −O–CH=C$\underline{H}_2$), 4.51–4.55 ppm (four singlets, Ph–C$\underline{H}_2$–O–), 6.49 (m, −O–C$\underline{H}$=CH_2), 7.32 (overlap with residual $CHCl_3$, 1H on $\underline{Ph}$–CH_2–O–), 7.38 (s, 4H on $\underline{Ph}$–CH_2–O–). ^{13}C NMR of Poly(EO-*co*-EGVGE) (125 MHz, $CDCl_3$): δ 61.6 (s, −$\underline{C}H_2$–OH of chain ends), 67.4 (s, −CH_2–CH(C$\underline{H}_2$–O–CH_2–CH_2–O–CH=CH_2)–O–), 69.8–72.6 (broad m, −$\underline{C}H_2$–$\underline{C}H_2$–O–$\underline{C}H_2$–CH(CH_2–O–C$\underline{H}_2$–C$\underline{H}_2$–O–CH=CH_2)–O–), 73,4 (s, Ph–$\underline{C}H_2$–O–), 77.2 (triplet, $\underline{C}DCl_3$), 78.6 (s, −O–CH_2–$\underline{C}$H(CH_2–O–CH_2–CH_2–O–

CH=CH_2)–O–), 86.7 (s, −O–CH=$\underline{C}H_2$), 127.6/128.4 (doublet, 5C on $\underline{Ph}$–CH_2–O–), 151.8 (s, −O–$\underline{C}H=CH_2$).

Supplementary Material

Refer to Web version on PubMed Central for supplementary material.

Acknowledgments

This work was supported by the National Institutes of Health as a Program of Excellence in Nanotechnology (HHSN268201000046C) (JKS, CJH, and NAL). MW thanks The Netherlands Organization of Scientific Research (NWO) for funding through a Rubicon Fellowship. The MRL Central Facilities are supported by the MRSEC Program of the NSF under Award No. DMR 1121053 (BFL, KTD, and FAL); a member of the NSF-funded Materials Research Facilities Network (www.mrfn.org).

References

1. Knop K, Hoogenboom R, Fischer D, Schubert US. Angew Chem Int Ed. 2010; 49:2–23.
2. Kainthan RK, Janzen J, Levin E, Devine DV, Brooks DE. Biomacromolecules. 2006; 7:703–709. [PubMed: 16529404]
3. De Freitas JN, Nogueira AF, De Paoli MA. J Mater Chem. 2009; 19:5279–5294.
4. (a) Armand M. Adv Mater. 1990; 2:278–286.(b) Meyer WH. Adv Mater. 1998; 10:439–448. [PubMed: 21647973] (c) Wright PV. Electrochimica Acta. 1998; 43:1137–1143.(d) Zhuang X, Xiao C, Oyaizu K, Chikushi N, Chen X, Nishide H. J Polym Sci Part A: Polym Chem. 2010; 48:5404–5410.
5. (a) Kojima C, Yoshimura K, Harada A, Sakanishi Y, Kono K. J Polym Sci Part A: Polym Chem. 2010; 48:4047–4054.(b) Du W, Li Y, Nyström AM, Cheng C, Wooley KL. J Polym Sci Part A: Polym Chem. 2010; 48:3487–3496.(c) Ren Y, Jiang X, Liu R, Yin J. J Polym Sci Part A: Polym Chem. 2009; 47:6353–6361.(d) Rahm M, Westlund R, Eldsäter C, Malmström E. J Polym Sci Part A: Polym Chem. 2009; 47:6191–6200.(e) Keul H, Möller M. J Polym Sci Part A: Polym Chem. 2009; 47:3209–3231.(f) Saville PM, Reynolds PA, White JW, Hawker CJ, Frechet JMJ, Wooley KL, Penfold J, Webster JRP. J Phys Chem. 1995; 99:8283–8289.
6. Dimitriou MD, Zhou Z, Yoo H-S, Killops KL, Finlay JA, Cone G, Sundaram HS, Lynd NA, Barteau KP, Campos LM, Fischer DA, Callow ME, Callow JA, Ober CK, Hawker CJ, Kramer EJ. Langmuir. 2011; 27:13762–13772. [PubMed: 21888355]
7. Mangold C, Wurm F, Obermeier B, Frey H. Macromol Rapid Commun. 2010; 31:258–264. [PubMed: 21590899]
8. Obermeier B, Frey H. Bioconjugate Chem. 2011; 22:436–444.
9. Mangold C, Wurm F, Obermeier B, Frey H. Macromolecules. 2010; 43:8511–8518.
10. Obermeier B, Wurm F, Mangold C, Frey H. Angew Chem Int Ed. 2011; 50:7988–7997.
11. Erberich M, Keul H, Möller M. Macromolecules. 2007; 40:3070–3079.
12. Lee BF, Kade MJ, Chute JA, Gupta N, Campos LM, Fredrickson GH, Kramer EJ, Lynd NA, Hawker CJ. J Polym Sci Part A: Polym Chem. 2011; 49:4498–4504.
13. (a) Kade MJ, Burke DJ, Hawker CJ. J Polym Sci Part A: Polym Chem. 2010; 48:743–750.(b) Nilsson C, Malmström E, Johansson M, Trey SM. J Polym Sci Part A: Polym Chem. 2009; 47:5815–5826.(c) Rosen BM, Lligadas G, Hahn C, Percec V. J Polym Sci Part A: Polym Chem. 2009; 47:3931–3939.(d) Yu B, Chan JW, Hoyle CE, Lowe AB. J Polym Sci Part A: Polym Chem. 2009; 47:3544–3557.
14. Haag R, Kratz F. Angew Chem Int Ed. 2006; 45:1198–1215.
15. Gravert DJ, Janda KD. Chem Rev. 1997; 97:489–510. [PubMed: 11848880]
16. (a) Bergbreiter DE. Chem Rev. 2002; 102:3345–3384. [PubMed: 12371888] (b) Dickerson T, Reed N, Janda K. Chem Rev. 2002; 102:3325–3343. [PubMed: 12371887] (c) Bergbreiter DE, Tian J, Hongfa C. Chem Rev. 2009; 109:530–582. [PubMed: 19209941]

17. Koyama Y, Umehara M, Mizuno A, Itaba M, Yasukouchi T, Natsume K, Suginaka A, Watanabe K. Bioconjugate Chem. 1996; 7:298–301.
18. Koyama Y, Ito T, Matsumoto H, Tanioka A, Okuda T, Yamaura N, Aoyagi H, Niidome T. J Biomat Sci-Polym E. 2003; 14:515–531.
19. Vetvicka D, Hruby M, Hovorka O, Etrych T, Vetrik M, Kovar L, Kovar M, Ulbrich K, Rihova B. Bioconjugate Chem. 2009; 20:2090–2097.
20. Hrubý M, Konák C, Ulbrich K. J Appl Polym Sci. 2005; 95:201–211.
21. Vetvicka D, Hruby M, Hovorka O, Etrych T, Vetrik M, Kovar L, Kovar M, Ulbrich K, Rihova B. Bioconjugate Chem. 2009; 20:2090–2097.
22. Yoshihara C, Shew C-Y, Ito T, Koyama Y. Biophys J. 2010; 98:1257–1266. [PubMed: 20371325]
23. Hashimoto M, Koyama Y, Sato T. Chem Lett. 2008; 37:266–267.
24. Sakae M, Ito T, Yoshihara C, Iida-Tanaka N, Yanagie H, Eriguchi M, Koyama Y. Biomed Pharmacother. 2008; 62:448–453. [PubMed: 18255250]
25. Koyama Y, Yamashita M, Iida-Tanaka N, Ito T. Biomacromolecules. 2006; 7:1274–1279. [PubMed: 16602749]
26. Koyama Y, Ito T, Matsumoto H, Tanioka A, Okuda T, Yamaura N, Aoyagi H, Niidome T. J Biomat Sci-Polym E. 2003; 14:515–531.
27. Yoshikawa K, Yoshikawa Y, Koyama Y, Kanbe T. J Am Chem Soc. 1997; 119:6473–6477.
28. Hunt JN, Feldman KE, Lynd NA, Deek J, Campos LM, Spruell JM, Hernandez BM, Kramer EJ, Hawker CJ. Adv Mater. 2011; 23:2327–2331. [PubMed: 21491513]
29. Shostakovskii MF, Atavin AS, Vyalykh EP, Trofimov BA, Tatarinova AF. Zhurnal Organicheskoi Khimii. 1967; 3(11):1972–1976.
30. (a) Shaikhutdinov EM, Karzhaubaeva RG, Osadchaya EF, Budanova TL. v sb Khimiya i Khim Tekhnol Alma-ata. 1974; 16:122–125.(b) Minakova TT, Usmanova TA, Brodskaya EI, Trofimov BA. Vysokomolekulyarnye Soedineniya, Seriya A. 1976; 18(2):469–471.
31. Mangold C, Dingels C, Obermeier B, Frey H, Wurm F. Macromolecules. 2011; 44:6326–6334.
32. Pang X, Jing R, Huang J. Polymer. 2008; 49:893–900.
33. Wilms D, Schoemer M, Wurm F, Hermanns MI, Kirkpatrick CJ, Frey H. Macromol Rapid Commun. 2010; 31:1811–1815. [PubMed: 21567598]
34. Heatley F, Yu G, Booth C, Blease TG. Eur Polym J. 1991; 27:573–579.
35. Garst J. Acc Chem Res. 1971; 4:400–406.
36. Crivello J, Kim W. J Polym Sci Part A: Polym Chem. 1994; 32:1639–1648.
37. Odian, G. Principles of Polymerization. 3. John Wiley & Sons; 1991. p. 452-523.
38. Frisch, MJ.; Trucks, GW.; Schlegel, HB.; Scuseria, GE.; Robb, MA.; Cheeseman, JR.; Montgomery, JA., Jr; Vreven, T.; Kudin, KN.; Burant, JC.; Millam, JM.; Iyengar, SS.; Tomasi, J.; Barone, V.; Mennucci, B.; Cossi, M.; Scalmani, G.; Rega, N.; Petersson, GA.; Nakatsuji, H.; Hada, M.; Ehara, M.; Toyota, K.; Fukuda, R.; Hasegawa, J.; Ishida, M.; Nakajima, T.; Honda, Y.; Kitao, O.; Nakai, H.; Klene, M.; Li, X.; Knox, JE.; Hratchian, HP.; Cross, JB.; Bakken, V.; Adamo, C.; Jaramillo, J.; Gomperts, R.; Stratmann, RE.; Yazyev, O.; Austin, AJ.; Cammi, R.; Pomelli, C.; Ochterski, JW.; Ayala, PY.; Morokuma, K.; Voth, GA.; Salvador, P.; Dannenberg, JJ.; Zakrzewski, VG.; Dapprich, S.; Daniels, AD.; Strain, MC.; Farkas, O.; Malick, DK.; Rabuck, AD.; Raghavachari, K.; Foresman, JB.; Ortiz, JV.; Cui, Q.; Baboul, AG.; Clifford, S.; Cioslowski, J.; Stefanov, BB.; Liu, G.; Liashenko, A.; Piskorz, P.; Komaromi, I.; Martin, RL.; Fox, DJ.; Keith, T.; Al-Laham, MA.; Peng, CY.; Nanayakkara, A.; Challacombe, M.; Gill, PMW.; Johnson, B.; Chen, W.; Wong, MW.; Gonzalez, C.; Pople, JA. Gaussian 03, Revision C.02. Gaussian, Inc.; Wallingford CT: 2004.
39. McLean AD, Chandler GS. J Chem Phys. 1980; 72:5639–5648.
40. Becke AD. J Chem Phys. 1993; 98:5648–5652.Lee C, Yang W, Parr RG. Phys Rev B. 1988; 37:785–789.
41. Schlegel HB. J Comp Chem. 1982; 3:214–218.
42. (a) Stolarzewicz A. Makromol Chem. 1986; 187:745–752.(b) Hans M, Keul H, Möller M. Polymer. 2009; 50:1103–1108.

43. (a) Fischer T, Kinsinger JB, Wilson CW. J Polym Sci Part B: Polym Lett. 1966; 4:379–386.(b) Yamashita Y, Ito K, Ikuma S, Kada H. J Polym Sci Part B: Polym Lett. 1968; 6:219–225.(c) Rudin A, O'Driscoll KF, Rumack MS. Polymer. 1981; 22:740–747.

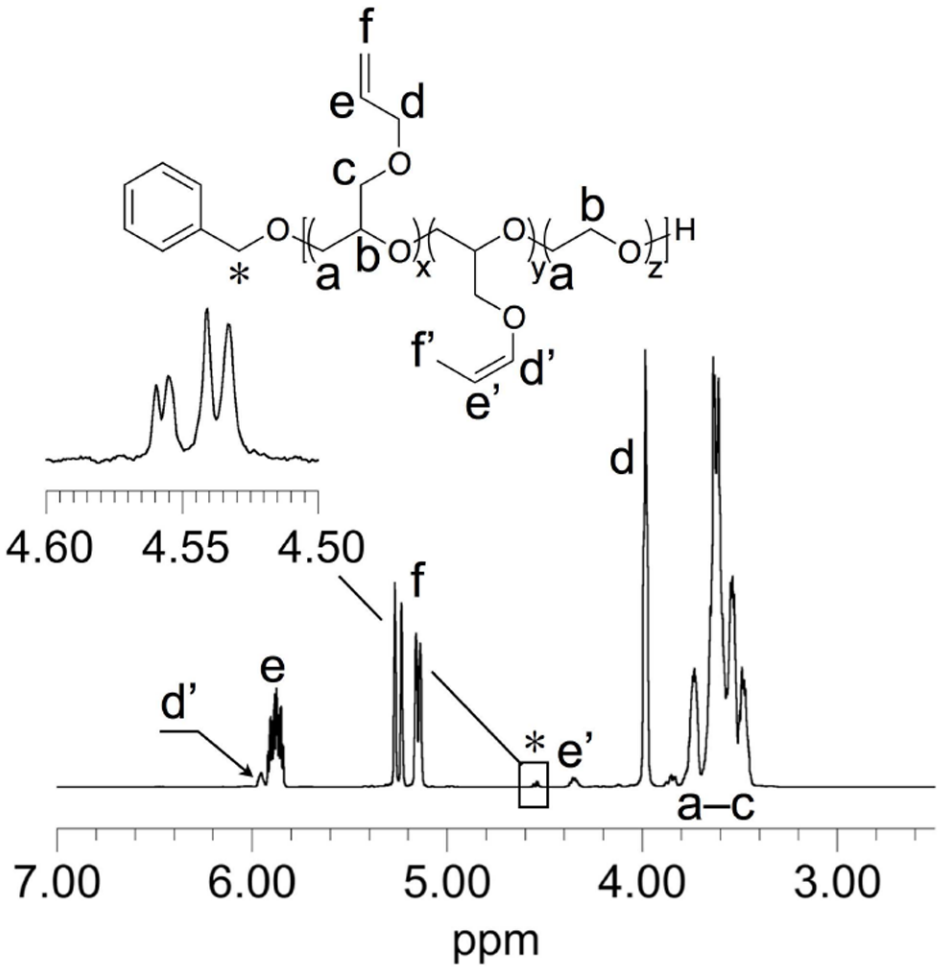

Figure 1.

^{1}H NMR spectrum of poly[(allyl glycidyl ether)-*co*-(ethylene oxide)] polymerized with $[EO]_0/[AGE]_0 = 1.0$. Inset shows the detail of the benzyl resonances (peak *).

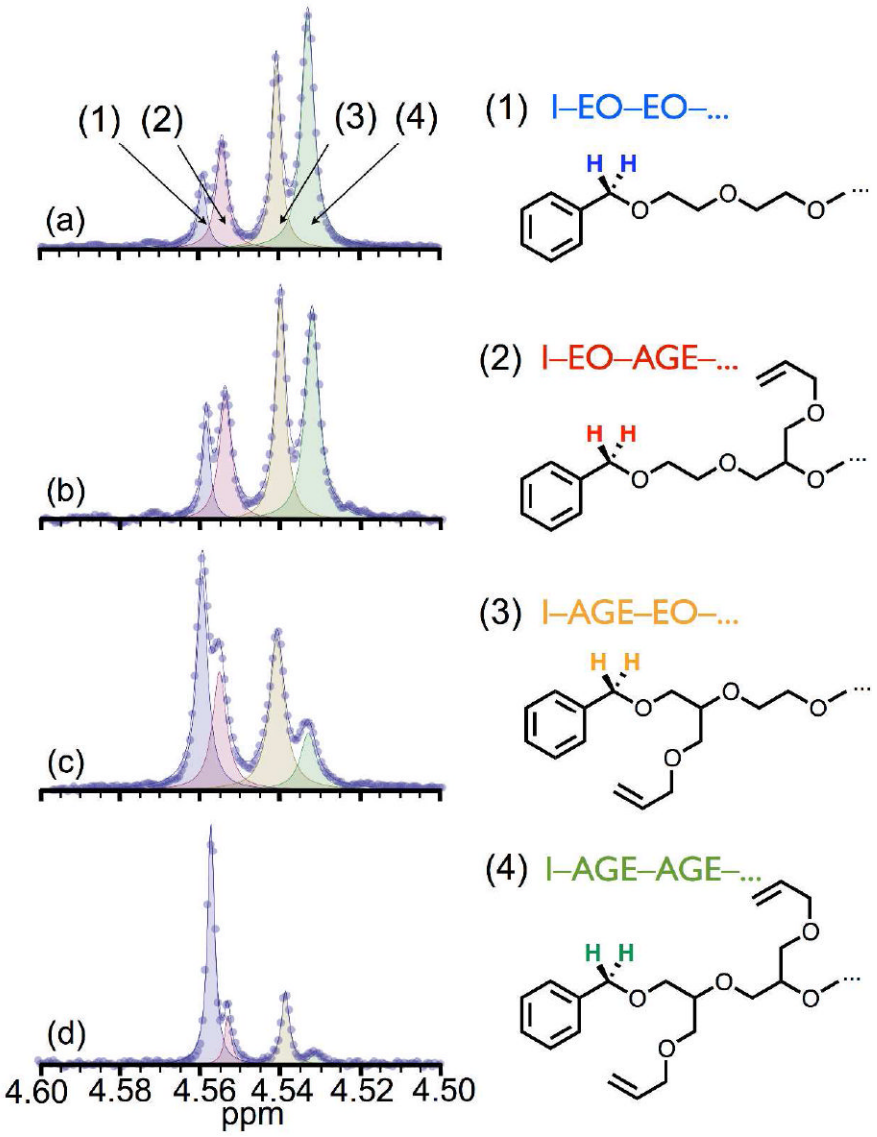

Figure 2.

^{1}H NMR spectra of the benzyl resonances (2H) for P(EO-*co*-AGE) with the following $[EO]_0/[AGE]_0$: (a) $[EO]_0/[AGE]_0 = 0.77$, (b) $[EO]_0/[AGE]_0 = 1.0$, (c) $[EO]_0/[AGE]_0 = 3.0$, and (d) $[EO]_0/[AGE]_0 = 7.5$. The ratios of integrals for these four $[EO]_0/[AGE]_0$ yield $k_G/k_E = 2.20 \pm 0.20$, $k_{G/G}/k_{G/E} = 1.31 \pm 0.26$, and $k_{E/G}/k_{E/E} = 1.86 \pm 0.10$, or $r_G = 1.31 \pm 0.26$ and $r_E = 0.54 \pm 0.03$ in terms of reactivity ratios.

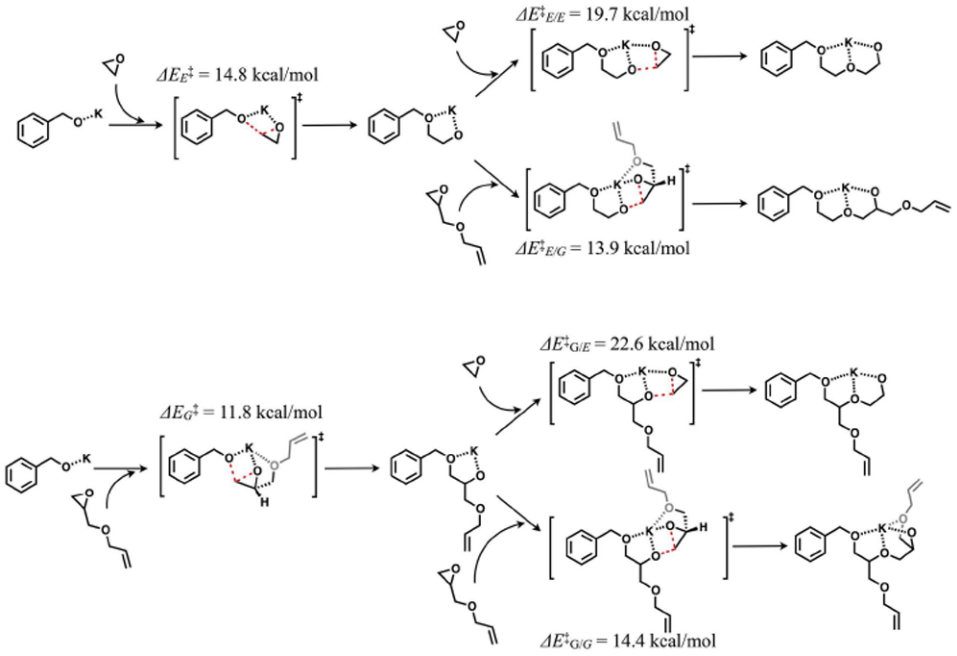

Figure 3.
Transition state structures and energies calculated by DFT for the first and second monomer additions. The transition state barrier for AGE addition is always lower than the corresponding EO addition.

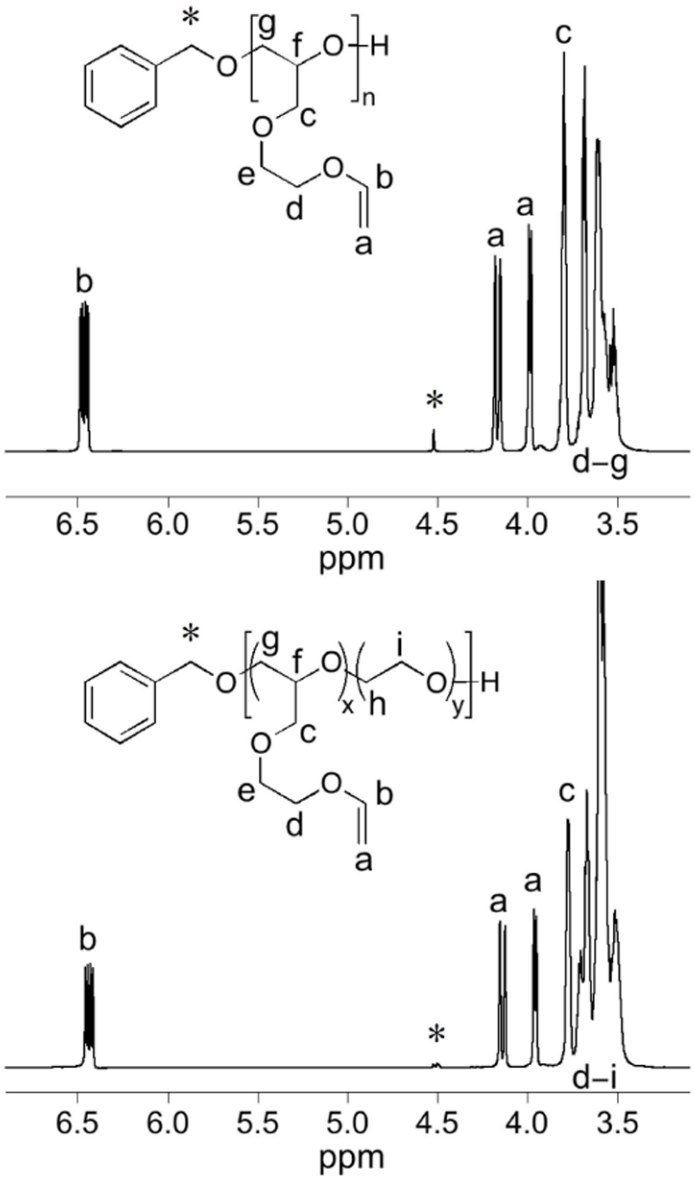

Figure 4.

^{1}H NMR spectrum of poly(EGVGE) (top spectrum) and poly(EGVGE-*co*-EO) (bottom spectrum). Peak assignments are shown in the inset. The peak near 4.5 ppm (peak *) is due to the benzyl (2H) end group protons used to determine molar mass. Compared with the homopolymer (top spectrum), the copolymer (bottom spectrum) shows a characteristic array of four singlets due to the benzylic protons correlated to the molar ratio of comonomers.

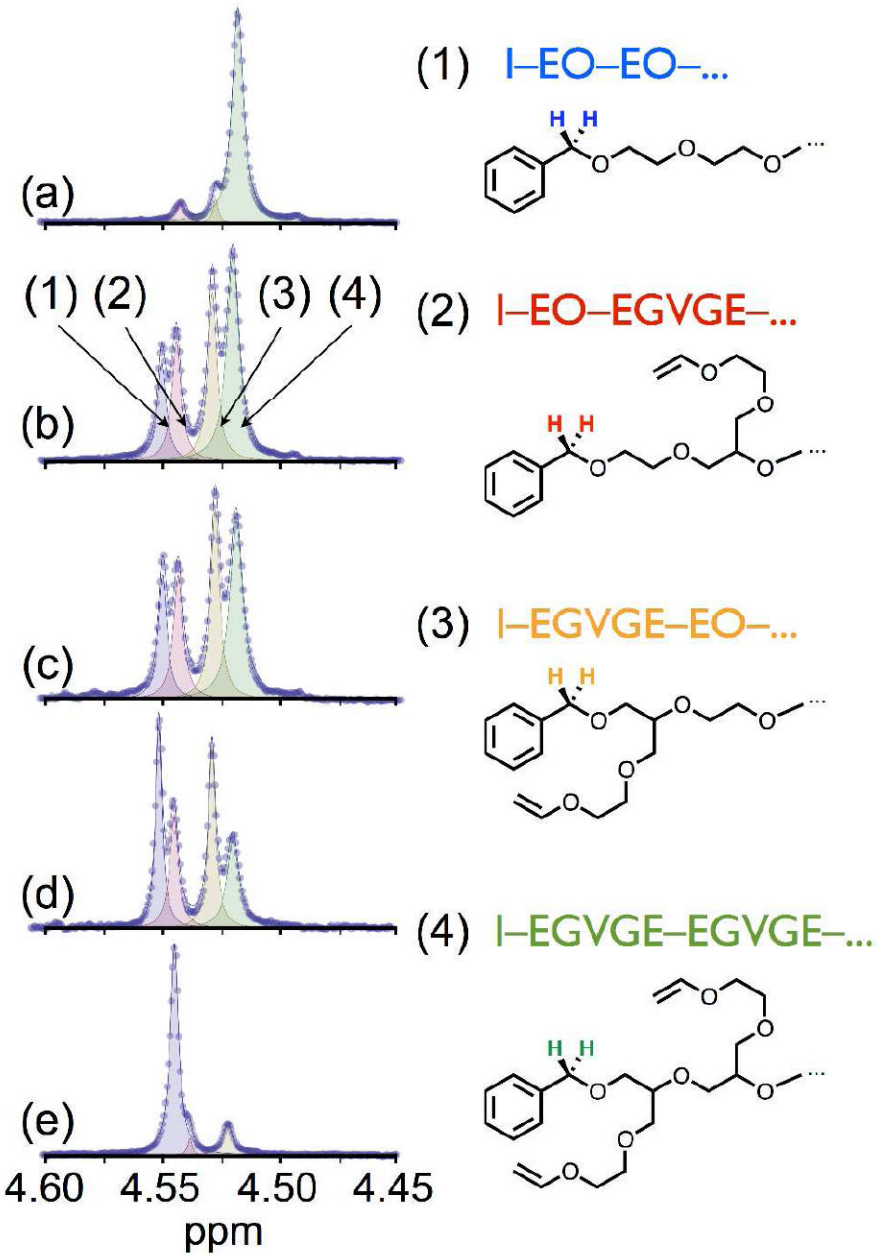

Figure 5.

^{1}H NMR spectra of benzyl resonances (2H) in d-chloroform. The relative peak intensities vary with the stoichiometric ratio of the two monomers in the copolymerization. $[EO]_0/[EGVGE]_0$: (a) 0.98, (b) 1.94, (c) 3.35, (d) 5.67, (e) 24.0. Using the integrals in b–d: k_G/k_E = 5.22 ± 1.30, $k_{G/G}/k_{G/E}$ = 3.50 ± 0.90, and $k_{E/G}/k_{E/E}$ = 3.30 ± 0.88, or r_G = 3.50 ± 0.90 and r_E = 0.32 ± 0.10.

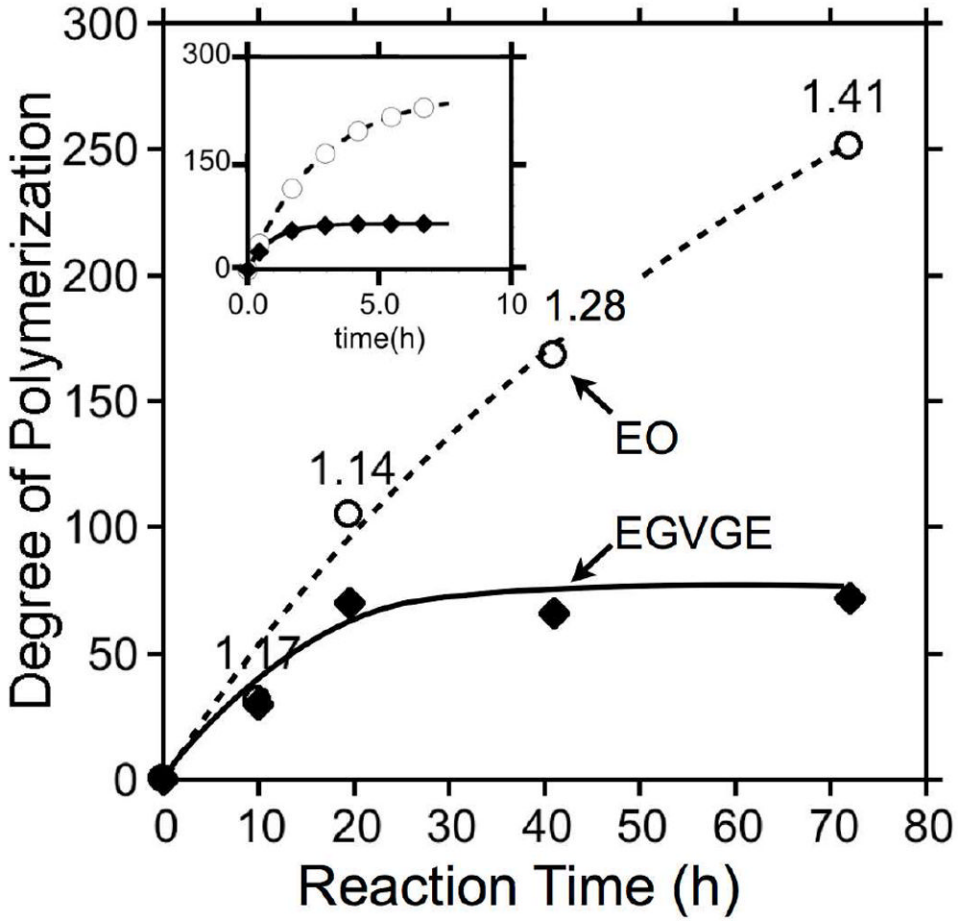

Figure 6.

Degree of polymerization of EO and EGVGE as a function of copolymerization time for several identically prepared copolymerizations. Polydispersity indices are shown alongside the data for each experimental time-point. Lines through the data serve as guides to the eye. Inset: Numerical calculation of degree of polymerization of comonomers (E, and G) with $[I]_0 = 0.01$, $[E]_0 = 250\times[I]_0$, $[G]_0 = 65\times[I]_0$, $k_{E/E} = 0.010\ M^{-1}\ s^{-1}$, $k_{E/G} = 0.030\ M^{-1}\ s^{-1}$, $k_{G/E} = 0.010\ M^{-1}\ s^{-1}$, $k_{G/G} = 0.035\ M^{-1}\ s^{-1}$: $r_G = 3.5$, $r_E = 0.33$.

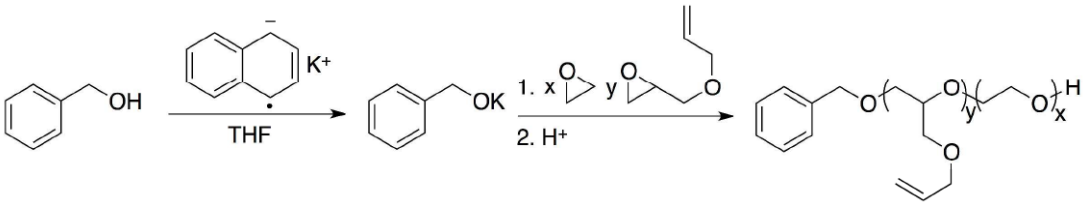

Scheme 1.
Copolymerization of ethylene oxide (EO) and allyl glycidyl ether (AGE) from a potassium alkoxide initiator.

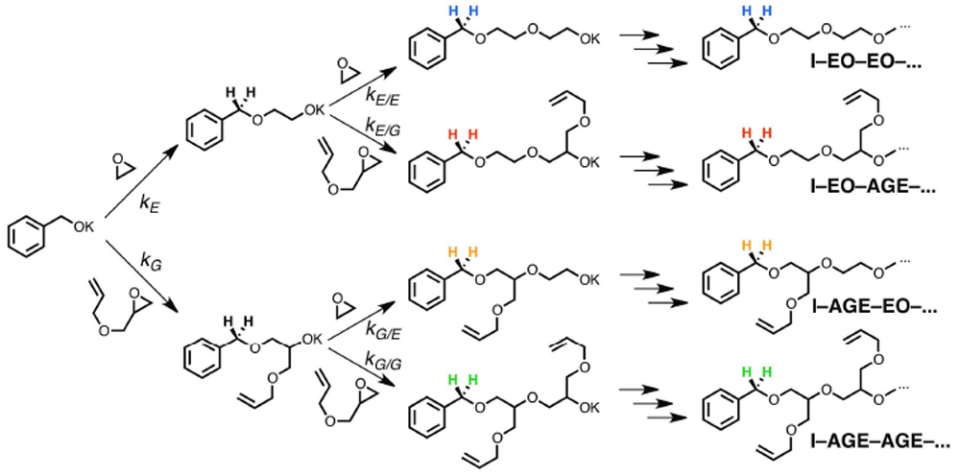

Scheme 2.

Kinetic scheme of initiation and the first propagation step for a copolymerization between ethylene oxide (EO) and allyl glycidyl ether (AGE) that results in four categories of copolymers differentiated by the sequence of the first two repeat units: I–EO–EO, I–EO–AGE, I–AGE–EO, and I–AGE–AGE.

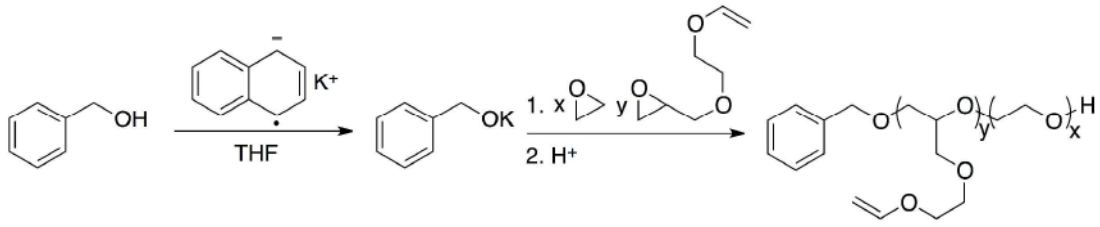

Scheme 3.
Copolymerization of EO and EGVGE.

Table 1

Poly[(allyl glycidyl ether)-*co*-(ethylene oxide)] copolymers synthesized at different molar ratios of comonomers.

No.	DP_{EO} [a]	DP_{AGE} [a]	PDI[b]	$[EO]_0/[AGE]_0$ [c]
1	690	81	1.12	7.45
2	83	24	1.09	3.00
3	200	160	1.11	1.00
4	130	140	1.09	0.77

[a] DP_{EO} and DP_{AGE} were determined by ^1H NMR spectroscopy using end-group analysis.

[b] Polydispersity indices were determined by SEC in chloroform relative to polystyrene standards.

[c] The ratio of initial monomer concentrations in the copolymerizations.

Table 2

Degree of polymerization (DP) and PDIs in homo- and co-polymerizations of EGVGE and EO after 20 h of copolymerization.

No.	EO		EGVGE		PDI[c]
	DP^{stoich} [a]	DP^{obs} [b]	DP^{stoich} [a]	DP^{obs} [b]	
1	227	236	-	-	1.05
2	227	236	10	10	1.13
3	227	220	42	44	1.17
4	227	104	69	70	1.14
5	136	64	69	60	1.25
6	68	56	69	66	1.17
7	-	-	69	60	1.21

All the polymerizations were carried out at a monomer concentration of 0.1g/ml in THF at 45 °C.

[a] DP^{stoich} was defined by the monomer to initiator ratio.

[b] DP^{obs} was measured by end-group analysis in ^{1}H NMR spectroscopy.

[c] Polydispersity indices were determined by SEC in chloroform relative to polystyrene standards.

Table 3

Degree of polymerization and molecular weight change during copolymerization of EO and EGVGE.

Reaction time (h)	EO		EGVGE		T_m [b] (°C)	ΔH_m [b] (J/g)	T_g [b] (°C)	PDI[c]
	DP[a]	Mn[a]	DP[a]	Mn[a]				
10	31	1,400	31	4,300	-	-	-61	1.18
19.5	105	4,600	70	10,100	-	-	-61	1.14
41	168	7,400	66	9,500	1	18	-60	1.28
72	251	11,100	72	10,400	34	33	-57	1.41

All polymerizations were carried out at the monomer concentration of 0.1g/ml in THF at 45°C.

[a] Degree of polymerization and molar mass were measured by NMR spectroscopy.

[b] T_m, ΔH_m and T_g were measured by DSC.

[c] Polydispersity indices were determined by SEC in chloroform relative to polystyrene standards.